

THE ELECTROMAGNETIC ENVIRONMENT IN CFC STRUCTURES

C J Hardwick and S J Haigh

Culham Lightning Test and Technology, Abingdon, Oxford, UK, OX14 3DB

ABSTRACT

Extensive measurements of induced voltages and currents have been made using a CFC horizontal stabilizer from the A320 as a test bed. The work was done to investigate the efficacy of various protection schemes to reduce the magnitudes of the induced voltages and validate a computer program INDCAL. Results indicate that a good understanding of the various induced voltage mechanisms including the long wave effect due to current redistribution has been obtained.

1 INTRODUCTION

The use of CFC in airframe construction produces indirect effects which have generated much interest in recent years. In particular, the relatively high resistivity of composite compared to aluminium leads to significant redistribution of current from the carbon fibre to any metallic components of the airframe during later times of the lightning waveform (References 1 and 2). This is because after the initial fast current rise, the di/dt magnitude decays and the current distribution is no longer inductively dominated.

In the latest FAA advisory circular AC20-136 (Reference 3), a long duration waveform, waveform 5 is specified for equipment tests to take account of the phenomenon. This current waveform, which will occur on conducting conduits or cable screens in hybrid structures (structures containing both metallic and CFC components) has a rise time of $50\mu s$ and time to $1/2$ height of $500\mu s$. Peak amplitudes specified are from 3-20kA.

This waveform 5 is supplementary to waveforms 1 and 4 which are current and voltage waveforms respectively which have the same shape as a component A lightning strike, waveform 2 which is the derivative of waveform 1 and waveform 3 which is a damped sinwave.

Some measurements on induced voltages and currents in a CFC horizontal stabiliser box were reported in a previous paper of this conference series (Reference 4); no protection was installed on the box resulting in conduit currents of up to 17kA, of a waveform 5 type due to current redistribution.

This present paper covers work investigating the effects of various protection methods such as aluminium strips bonded to the box and of surface coatings of metallic foil. Induced voltages were measured on wires routed inside and outside of conducting conduits, as well as the current distribution around the structure.

Section 2 describes the experimental configuration, Section 3 presents the results and Section 4 presents some limited comparisons with INDCAL (Reference 5) computer predictions. Section 5 makes predictions for more general hybrid structures.

The work has been supported by the Culham Lightning Club.

2 EXPERIMENTAL CONFIGURATION

The basic experimental configuration is shown in Figure 1 and this is similar to that used in the previous work reported in Reference 4. A 1.5m long metallic braided conduit was installed inside the stabiliser and linked two aluminium boxes both of which were well bonded to the CFC; induced voltage diagnostics were installed in one of the boxes. The extent of the aluminium protection strips and foil are also indicated in the figure. Figure 2 indicates the wire circuits on which the induced voltage measurements were made. Each wire was shorted to the metallic box at one end and terminated in a high impedance at the other end. In addition to the unprotected structure (Figure 2a), data for three different protection configurations were measured; these were:

A1 Strips

2.5cm wide, 2mm thick A1 strips bonded along their entire length with M4 screws using existing captive nuts. These nuts were present for attaching aluminium strips on the production aircraft (Figure 2b).

Foil

25 μ thick aluminium foil of resistivity 2.5m Ω /□ was placed over the upper and lower skins and extended as far as the entire length of the strips. The foil was clamped near the leading and trailing edges by the aluminium strips. It was isolated from the CFC surface by a layer of polythene - this was in order to ensure the current paths to the foil were well defined (Figure 2c).

Thin aluminium strip was also used to sandwich the foil edges to the CFC at its furthest inboard and outboard extent, and held down with several self tapping screws. This was to enable current to pass straight from the CFC to the foil without having to deviate to the aluminium strips at the leading and trailing edges first.

External Conduit

The 1.5m, conduit used hitherto was joined by a 360° joint to a similar piece of conduit giving a 3m long conduit of total resistance of 9.6m Ω . The ends of this assembly were again bonded to the termination boxes A and B with 360° joints, but the cable was routed external to, and its centre 4cm away from the front spar of the stabiliser (Figure 2d).

3 RESULTS

The measurements are tabulated in Table 1 for the unprotected configuration, Table 2 for the "strip" configuration, Table 3 for the "foil and strip" and Table 4 for the "external conduit". The data values have been linearly extrapolated to 200kA peak current, but were generally obtained with a driving waveform of 12kA peak current, rise time 1.3 μ s, time to 1/2 height on falling tail, 12 μ s. For a Component A driving waveform, because of the longer decay time (70 μ s), larger redistribution currents would be obtained.

The capacitor bank voltage was 120kV, which with the 2.2 μ H inductance of the structure gave a peak value of di/dt of 53kA/ μ s. Hence the appropriate scaling factors to 200kA peak current and 140kA/ μ s peak di/dt are 18 and 2.64 respectively.

INDCAL calculations were made using the cross section of the structure shown in Figure 2e and comparisons with data in the different configurations are made in Figures 3-6. The agreement is very favourable (3dB). Aspects of these waveforms are discussed in Section 4.

TABLE 1

	VALUE of Peak Current/Voltage at 200kA	RISE TIME μ s
Current at box corner	11.87 kA	1
Upper skin	7.85 kA	1.7
Lower skin	7.15 kA	2.0
Lower skin density * resistivity x 1.5m	1185 V	
ICORE current	17.25 kA	23
ICORE current x 3.8m Ω (ICORE resistance)	66 V	
Inner wire voltage	52 V	24
Outer wire voltage	109 V	2.6
Inner, ICORE disconnected	1500 V	2.5

TABLE 2
2.5cm A1 strips installed + ICORE

	VALUE AT 200kA	RISE TIME μ s
Strip current	21 kA	4
Upper skin	7.3 kA	2
Lower skin	6.6 kA	2
Density x resistivity x 1.5	1110 V	
ICORE	11.8 kA	20
ICORE current x 3.8m Ω	44 V	
ViR inner	46 V	18
Difference dB	0.4	
ViR outer	90 V	2.5

TABLE 3
Strips and foil installed

	VALUE AT 200kA	RISE TIME, μ s
Strip current	18 kA	
Upper skin	7.3 kA	2
Lower skin	6.2 kA	2
Density x resistivity x 1.5m	206 V	
ICORE	8.5 kA	30
ICORE current x 3.8m Ω	32 V	
ViR inner	33 V	26
ViR outer	54 V	4
ICORE current x 3.8m Ω	32 V	

TABLE 4
ICORE routed outside

	VALUE AT 200kA	RISE TIME, μ s
Strips	16 kA	2.5
Upper skin	7.1 kA	2
ICORE	7.6 kA	2
ICORE current x 9.6m Ω	77 V	2.5
ViR inner	90 V	.8
ViR outer	94 (648)V ⁺	~ .1
ViR outer ICORE disconnected	7.9 kV	

Notes:

- + Bracketed figure is figure that would be obtained by scaling di/dt by same factor as current
For waveforms with high HF content we have scaled to peak di/dt (factor 2.6) not current (x18) as
the coupling mechanism is proportional to di/dt rather than current.

4 DISCUSSION

Measurements of voltages on wires in many different internal positions were made in addition to those illustrated in Figure 2, however space precludes their inclusion; details are available in the Culham Lightning Club reports (Reference 6). Nevertheless the agreement with INDCAL predictions for voltages was generally within about 6dB and the trend of values and waveshapes is shown in Figure 7. These trends can be understood in terms of the resistive voltage drop and diffusion flux penetration through the box walls.

Circuits using the box structure as a return path will have an induced voltage due to the sum of the resistive voltage drop along the structure itself plus a contribution from the rate of change of flux threading the circuit of wire and structural return. Well inside the CFC structure and away from any apertures this will be diffusion flux whose rate of change, roughly follows the current wave shape. Depending on direction of the flux it may add or subtract to the structural voltage. At conducting elements in the box, the structural/diffusion flux voltage will drive redistribution current into the conduit; this current will in turn reduce the total flux near to the conduit.

The relative screening offered by the different configurations have been summarised in Figure 8. The results have been derived from the peak voltage data from the tables normalised to 1A, or to 140kA/ μ s/200kA depending on the coupling mechanism, to give a screening figure of merit in dB Ω . Shown on the same graph are the AC20-136 threat levels. Computations show that with an AC20-136 component A driving waveform (longer than our experimental waveform) the values of induced voltage on wires inside the conduit which carry a redistribution current would be 7dB higher. Hence with a component A waveform, the ICORE routed inside gives a waveform 5 type of induced voltage 3dB below level 2 (redistribution will effect peak value and 7dB correction added). The externally routed ICORE would give a waveform 4 type of induced voltage, 3dB below level 2 (redistribution current will not effect peak value which occurs with the peak of the driving current and no correction made). For longer cables 6dB should be added for each doubling of length. Computer studies (see next section) have shown that provided the resistance per unit length of the conduit is not too high the current is largely determined by the CFC resistance and structure geometry which leads to the induced voltage developed being roughly proportional to conduit resistance. Differential voltages on two

wire circuits of course would be some 20dB lower. Simple computations like these can thus be used to define the shapes and magnitudes of currents and voltages on circuits in the structure that will occur.

Detailed comparisons between data and predictions are now discussed:-

a) **BASIC STRUCTURE**

The current density at the corners of the wing box, near to the position of the aluminium strips is initially higher than elsewhere but decays more quickly than for example the current on the top skin. This is understood in terms of an initial inductive current distribution followed by resistive redistribution. The INDCAL/data comparison is made in Figure 4.

b) **STRIPS**

As expected the Aluminium strips drain current from the structure at late times so the strip current waveform is higher in amplitude and shows a much later zero crossing than the current measured in the carbon fibre at the same position before the strips were installed.

Moreover as the strips are more conductive than the ICORE current redistributes into them more readily and the ICORE current has a lower amplitude (-3dB) and decays earlier. Figure 5 shows that INDCAL is accurate to within 3dB.

Due to flux generated by redistribution current flowing in the conduit (whose rate of change is proportional to structure current) threading between the "outer" wire and the ICORE, the "outer" voltage is higher than the inner and has a shorter time to peak.

c) **FOIL**

Since the average resistivity of the skin has been reduced considerably the redistribution out of the skin and into the strips is not now so marked. Consequently the strip current is less and decays more quickly. The diffusion flux takes longer to penetrate the more conductive skin and hence. The current in the ICORE now has a longer rise time and its amplitude is reduced by a further 2dB compared to the "strips only" configuration. A comparison with INDCAL is made in Figure 6 and again agreement with INDCAL is good.

It was difficult to make a good joint between the foil and the CFC, and the joint resistance was substantial compared to the $2.5\text{m}\Omega/\square$ foil resistance. Since the ICORE current is a sensitive function of the foil resistivity the computation includes a value of foil resistivity that takes account of the measured joint resistance. INDCAL predicted an ICORE current of 3% for an effective skin resistivity of $4\text{m}\Omega/\square$, which is close to the observed value of about 4%.

The "outer" wire voltage has been reduced by a larger factor (6dB) by the addition of foil than by the addition of strips since the diffusion flux penetrating to the interior will be lower due to the lower effective skin resistance. Hence foil is very effective at reducing common mode resistive voltage that would occur on unscreened wires in CFC structures.

d) **EXTERNAL CONDUIT**

The flux driving the current into the conduit is mainly fast aperture flux threading between the ICORE and structure so the current waveform follows more nearly the driving waveform except it remains higher at late times due to current redistribution. INDCAL predictions are shown in Figure 7 together with measured values. The computation includes a reduced cross section for the conduit to give a 50% increase in the self inductance of the ICORE (The ICORE conduit is longer than the length of structure it spans). Because of the large amplitude of di/dt of the current in the conduit there is a big difference between inner and outer voltages.

5 COMPUTATIONAL STUDY

To find how the redistribution currents were affected by the variation of several parameters some computational studies were made. Table 5 shows the result of such a study on a box of similar cross section and make up to the experimental structure. As the resistivity of the structure and hence total resistance is lowered (a similar effect would result from increasing the size of the box) the peak current in the conduit takes a longer time to reach peak but the magnitude decreases rapidly. As the resistance of the conduit becomes lower, its current also increases as does the time to peak but it is limited eventually by its inductance and these are a range of values below which the conduit current does not vary greatly.

More studies of different structures indicated that in general the more important parameters, are the CFC resistivity as noted in this section and the relative proportion of CFC to metal as noted in Section 4b). A range of rise times and fall times for the long wave are possible and the 50 μ s/500 μ s is only one example of the form of redistribution currents, longer and shorter waveforms can occur. In particular if a substantial proportion of the structure is a poorly conducting metal such as would be found in a CFC covered titanium engine, very long pulses due to redistribution from the titanium to a good conducting conduit could be produced.

TABLE 5
Computational results for box with strips and foil

BOX RESISTIVITY M Ω /□	ICORE RESISTANCE m Ω	ICORE %	CURRENT RISE TIME μ s
2	4.8	4.8	90
4	4.8	7.6	70
6	4.8	9.5	58
4	2.4	8.5	80
4	9.6	6.5	60
4	48	3.2	35

6 CONCLUSIONS

6.1 A resistive INDCAL analysis gives a good understanding of the induced voltage and current redistribution mechanism in hybrid structures. The agreement on the structure studied was within 3dB for currents in the structure and 6dB for voltages.

6.2 The most severe common mode voltages inside hybrid structures are of the order of the maximum resistive voltage drop and these occur for wires routed near the composite skin particularly skin with high curvative; for other wires the voltage will in general be lower especially those routed near to internal low resistance current carrying conductors.

Currents on internal conduits will have long rise times and the induced voltage waveform of a wire inside a 360° bonded conduit follows the current waveform precisely and has a magnitude equal to the conduit current x DC resistance.

6.3 Computational predictions show that the current carried by conduits or cable shields within a hybrid structure has a peak magnitude and a rise time-to-peak which is dependent on several factors relating to the geometry and resistivity of the skin and internal structure; the more important factors being the relative proportion of metal to CFC in the outer skin and the CFC resistivity.

7 REFERENCES

1. A Plummer et al. The Behaviour of Electric Currents in Graphite/Epoxy Structures. ICOLSE 1988, Oklahoma, USA.
2. C Jones. The Slow Equipment Test Waveform for Systems in CFC Structures. ICOLSE 1989, Bath, UK.
3. FAA AC20-136, Protection of Aircraft Electrical/Electronic Systems against the Indirect Effects of Lightning, 1991.
4. C Hardwick et al. Induced Effects Associated with Lightning Strikes to Hybrid Structures. ICOLSE 1989, Bath, UK.
5. C Hardwick et al. A Filamentary Method for calculating Induced Voltages within Resistive Structures in either the Frequency Domain or Time Domain. ICOLSE 1988, Oklahoma, USA.
6. C Hardwick et al. The Electromagnetic Environment Inside the CASA CFC Horizontal Stabilizer. Culham Lightning Club Report 6-13.

8 ACKNOWLEDGEMENTS

The authors would like to acknowledge financial support from the Culham Lightning Club; comprising: British Aerospace, Rolls Royce, Westlands, CASA, SAAB, Shorts, CAA, DTI.

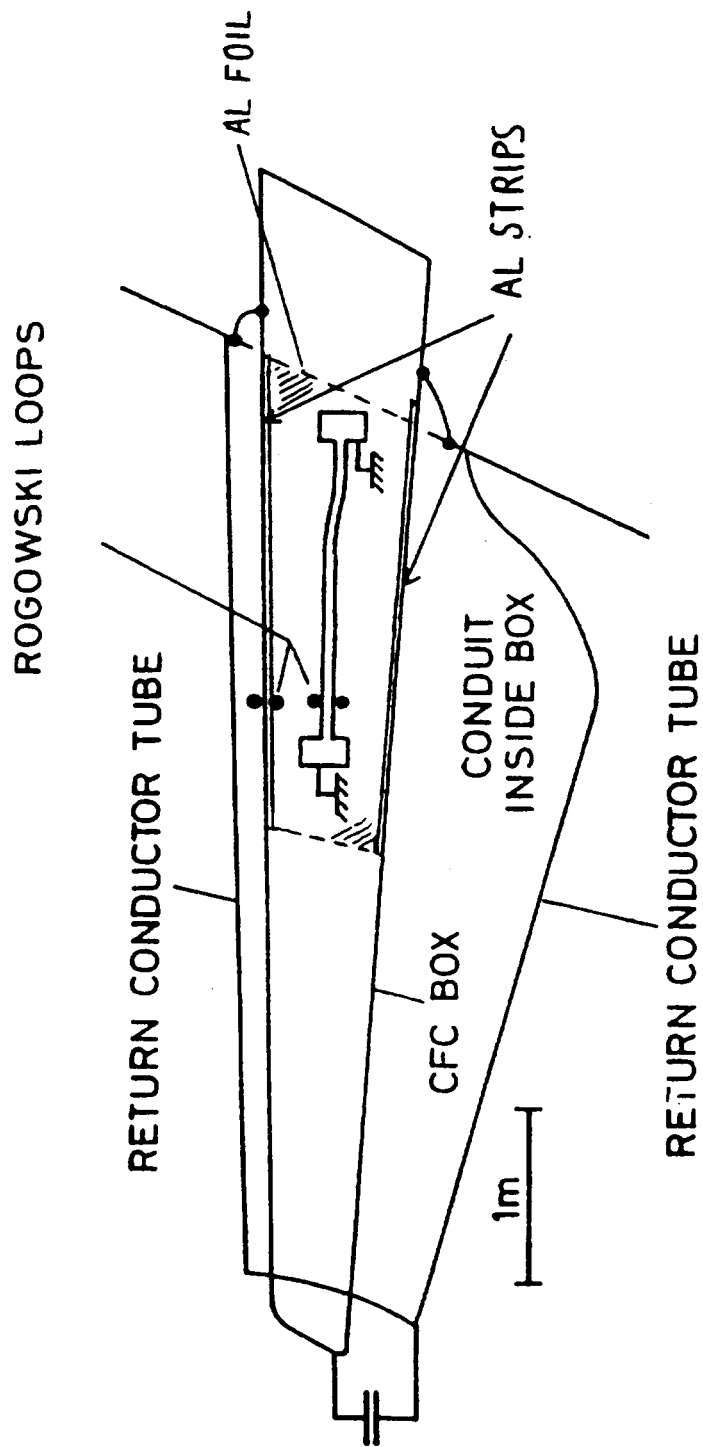
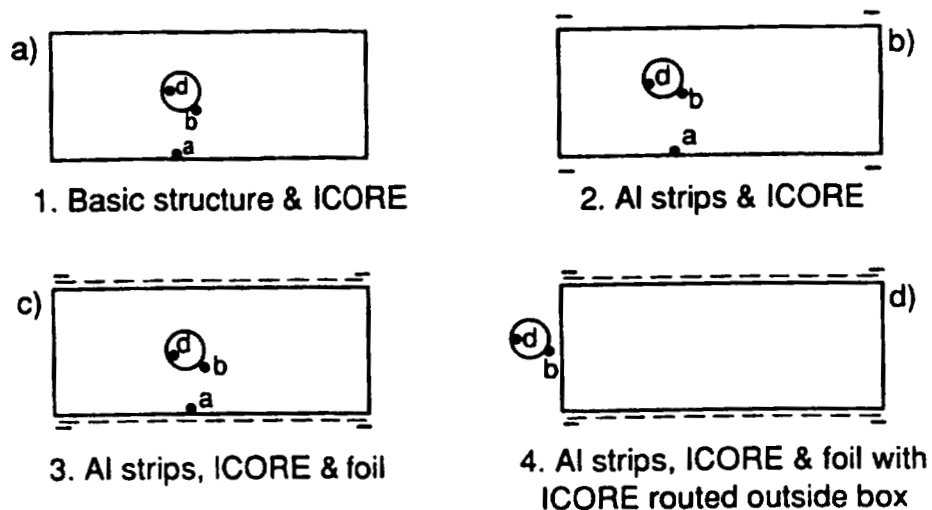


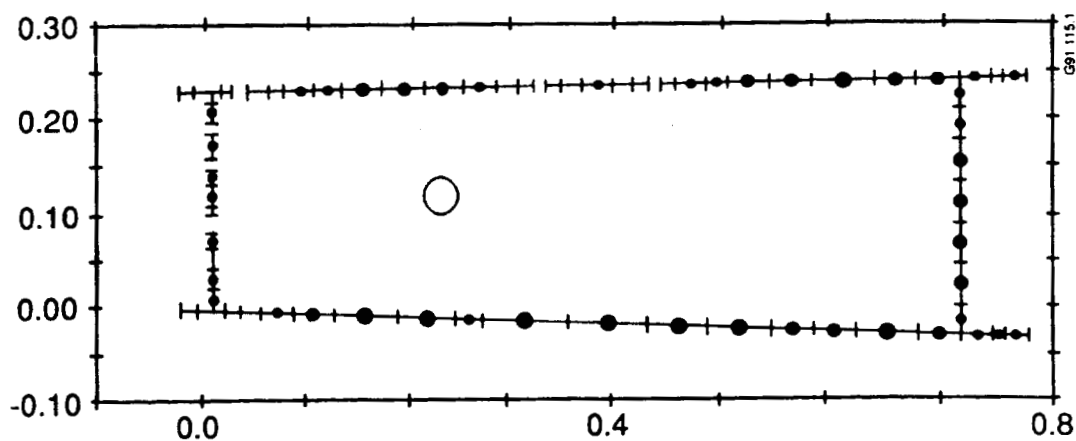
FIG 1 Plan view of A320 horizontal stabilizer central box section.

Figure 2: Different configurations whose results are plotted in figure 8



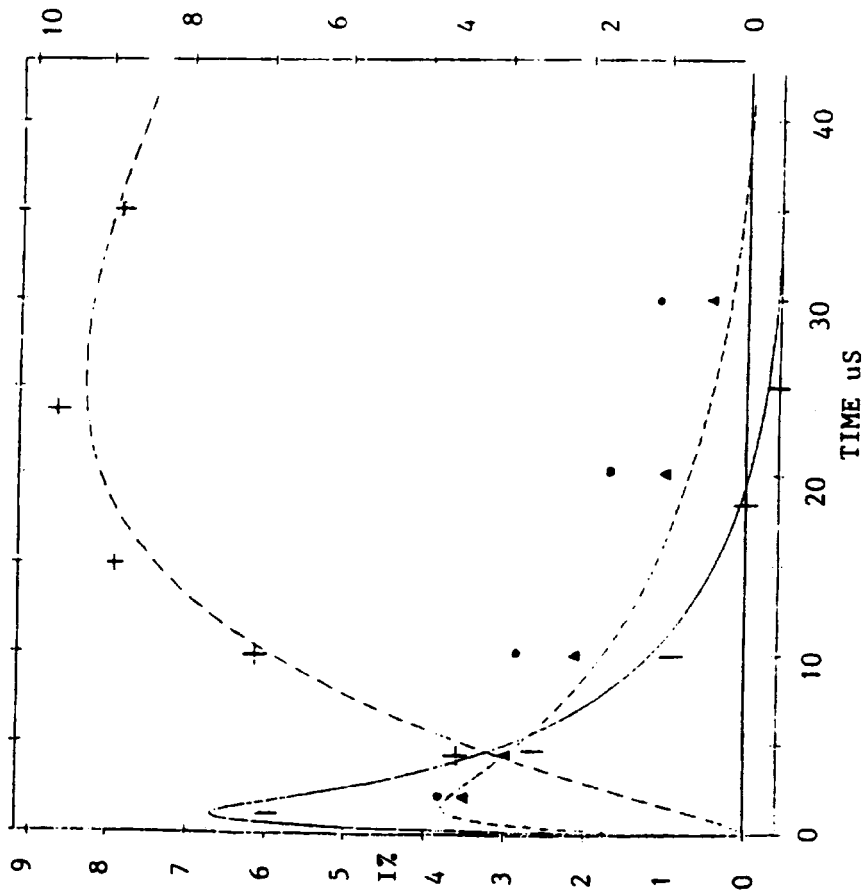
Key : Wire a - Structural return
 b - External to ICORE
 d - Internal to ICORE

For configuration 4 datum for structural return plotted in figure 8 is for wire d with the ICORE disconnected



e) Typical filamentary representation for INDICAL

FIG 3 BASIC STRUCTURE RESULTS

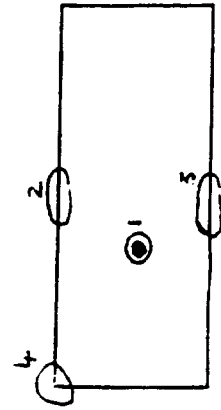
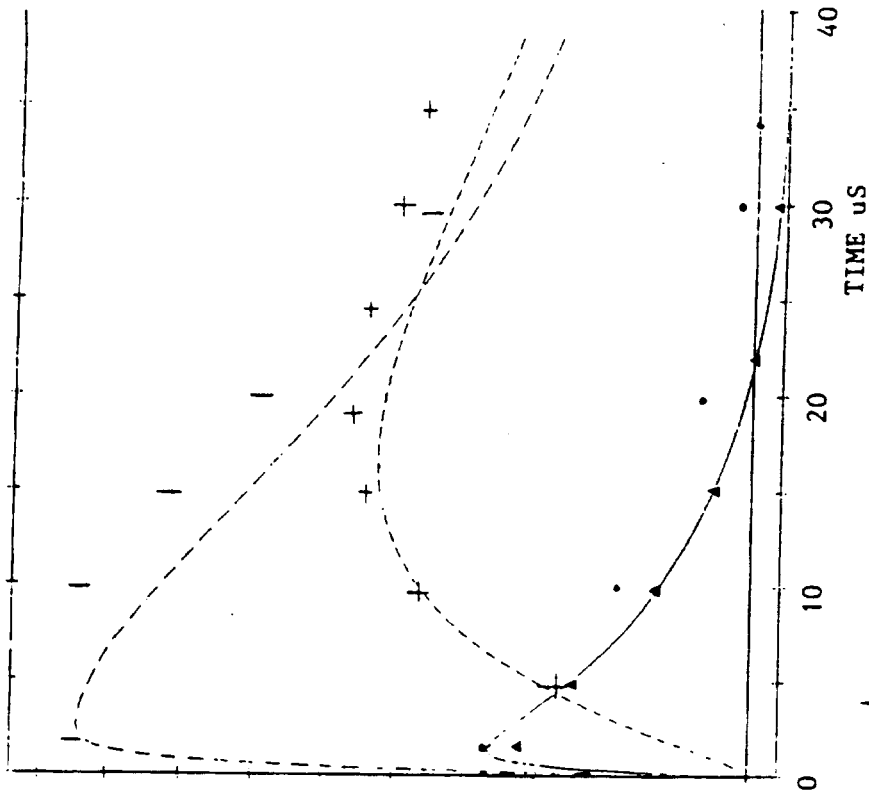


KEY FOR FIGS 3-6

Diagram opposite shows a section through the stabilizer box showing the positions of the current measurements. The data are plotted with the corresponding symbol and the INDICAL predictions are plotted as lines

- 1 CONDUIT
- 2 UPPER SKIN
- 3 LOWER SKIN
- 4 BOX CORNER

FIG 4 STRUCTURE WITH STRIPS RESULTS



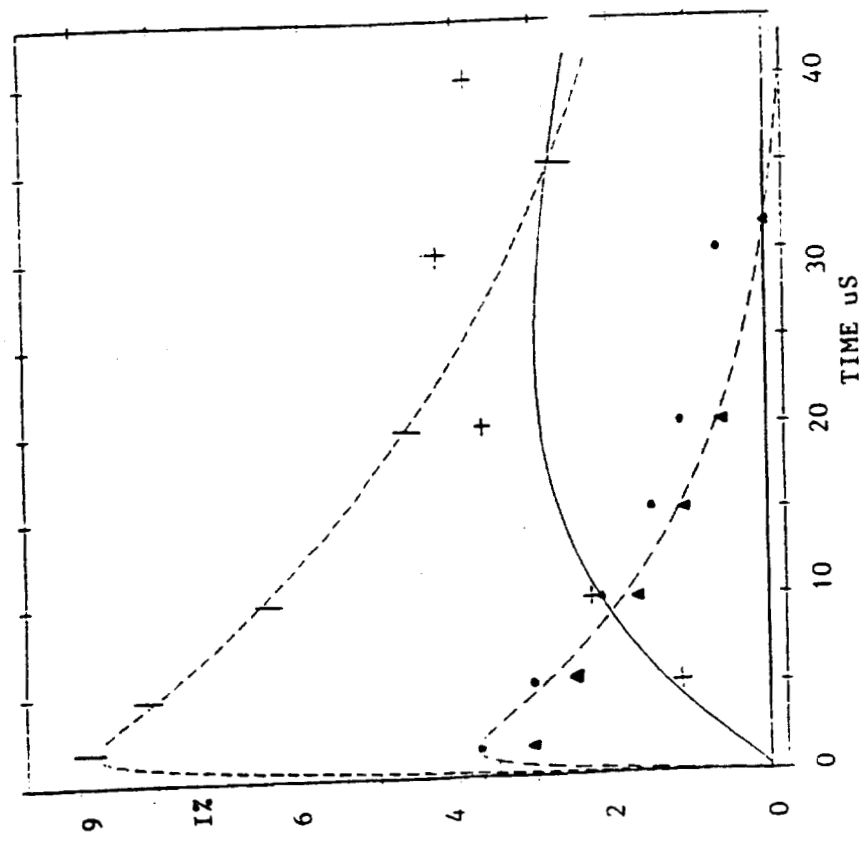


FIG 5 STRUCTURE WITH STRIPS & FOIL
KEY as FIGS 3 & 4

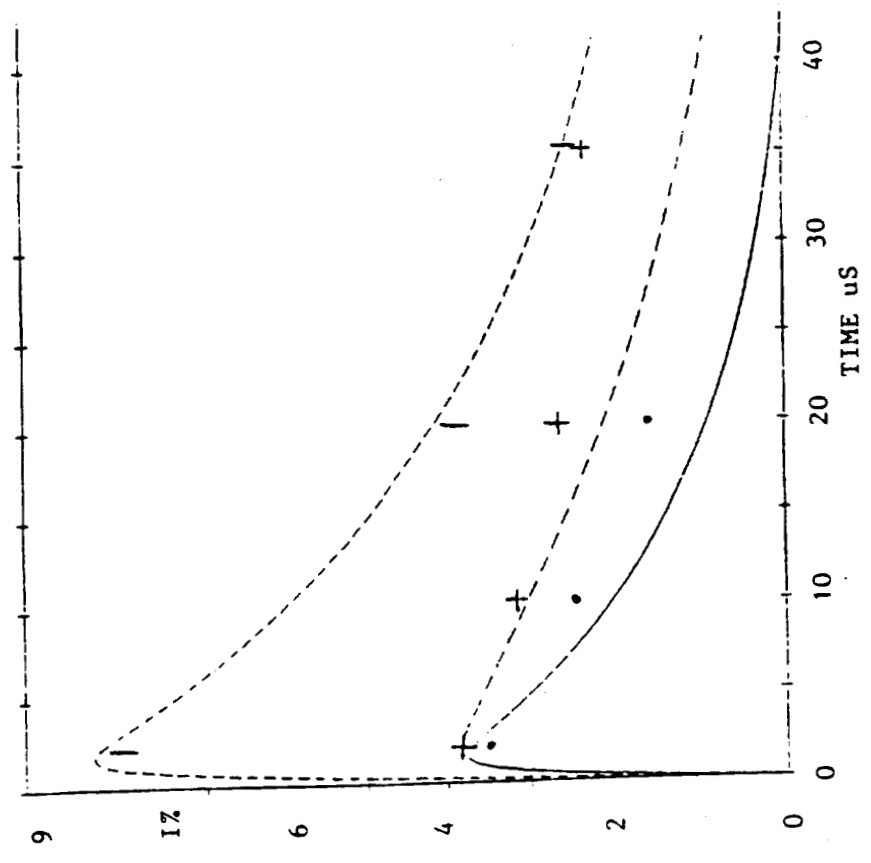


FIG 6 STRUCTURE WITH EXTERNAL CONDUIT

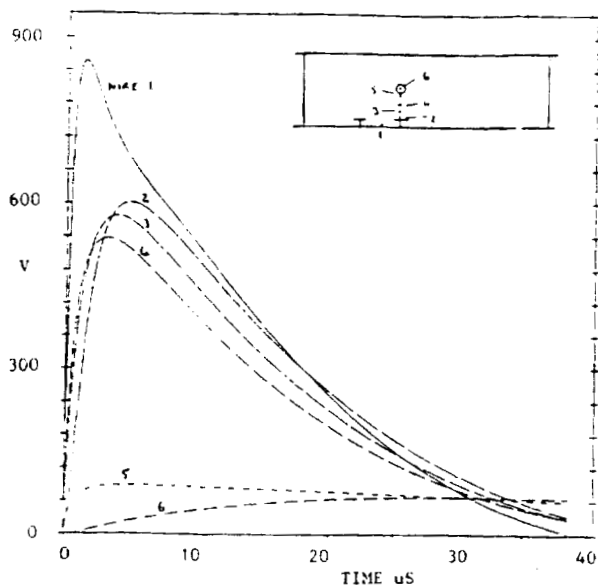


Figure 7: Voltage waveforms for wires at different positions as shown in insert. The longer rise times for the wires 2-4 are due to current taking time to penetrate to the internal structure

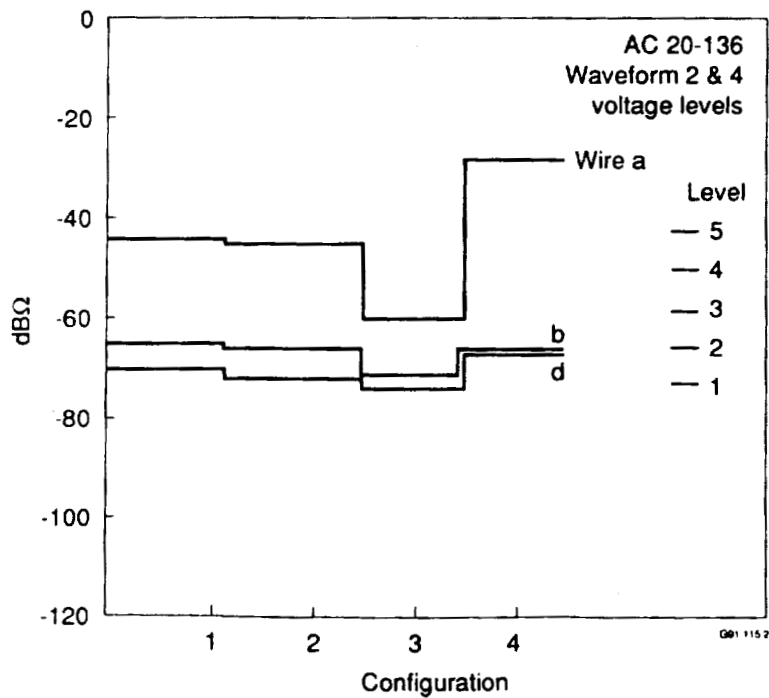


Figure 8: Time domain peak voltage data from tables 1 to 4 plotted relative to driving current in dBΩ